

Efficient tuning of electroluminescence from sky-blue to deep-blue by changing the constitution of spirobenzofluorene derivatives

Houjie Liang^{a,c}, Xinxin Wang^b, Xingye Zhang^{a,c}, Ziyi Ge^{a,*}, Xinhua Ouyang^{a,*}, Suidong Wang^{b,*}

^a Ningbo Institute of Materials Technology & Engineering, Chinese Academy of Sciences, Ningbo 315201, PR China

^b Institute of Functional Nano & Soft Materials, Soochow University, Suzhou 215123, PR China

^c University of Chinese Academy of Sciences, Beijing 100049, PR China

ARTICLE INFO

Keywords:

Spiro[benzofluorene-fluorene]
Spiro[benzoanthracene-fluorene]
Constitution
Blue OLED
Color purity
Nondoped system

ABSTRACT

Two novel benzimidazole-attached spiro[benzofluorene] derivatives, 2,2'-(spiro[benzo[c]fluorine-7,9'-fluorene]-5,9-diylbis(4,1-phenylene))bis(1-phenyl-1*H*-benzo[d]imidazole) and 2,2'-(spiro[benzo[de]anthracene-7,9'-fluorene]-2',3-diylbis(4,1-phenylene))bis(1-phenyl-1*H*-benzo[d]imidazole), were prepared by a Suzuki coupling reaction. Their photophysical and photochemical properties were studied systemically. The fluorescent organic light-emitting diodes were fabricated by using them as the emitters, all of them showed strong blue emission. Interestingly, from the benzoanthracene derived compound a high color purity was found with Commission de L'Eclairage 1931 chromaticity coordinates of (0.15, 0.10) and an efficiency of 1.96 cd/A. To the best of our knowledge, this is the first time to obtain a deep-blue emission with spiro[benzofluorene] derivative in a nondoped device.

1. Introduction

Blue organic light-emitting diodes (OLEDs) have been attracting great scientific and commercial attention for their potential applications in both full-color display and solid-state lighting [1–4]. Much significant progress has been demonstrated and the external quantum efficiencies (EQE) over 20% have been accessible for phosphorescent OLEDs (PhOLEDs) and more than 10% for fluorescence. However, it is still particularly difficult to generate a deep-blue emission with Commission Internationale de l'Eclairage (CIE) coordinates in the range of ($CIE_x < 0.15$, $CIE_y < 0.15$) due to the intrinsic wide band gap nature of deep-blue emitters [5–7]. Although great effort has been made to develop deep-blue fluorescent emitters in the past decade, there is still a clear need to improve the color purity and stability of deep-blue OLEDs.

Spirofluorene and their derivatives as important intermediates have attracted great interest due to their special structures and properties. In 2008, Gong et al. introduced asymmetric

spirobenzofluorenes containing naphthalene groups into OLEDs, the results indicated good stabilities, high carrier mobilities and high fluorescence quantum yields [8]. Subsequently, Huang et al. reported series of novel spirobenzofluorene/pyrene derivatives as dopant materials and obtained deep-blue emission [9]. Recently, Gong et al. demonstrated one of spirobenzofluorene dimers as host materials and the maximum efficiency was up to 7.44 cd A⁻¹ with deep-blue emission [10]. However, the reported results based on spirofluorene derivatives showed that most examples were used as host or dopant materials. It is well-known that the electroluminescent properties are extremely sensitive to the dopant concentration and very difficult to control by using co-deposition methods [11–13]. Furthermore, the energy transformation may be ineffective because of the potential phase separation in host-dopant system [14]. Therefore, to develop the nondoped, highly efficient, deep-blue emitters based on spirobenzofluorene derivatives is attractive.

In this study, we designed and synthesized two novel blue emitting materials, 2,2'-(spiro[benzo[c]fluorine-7,9'-fluorene]-5,9-diylbis(4,1-phenylene))bis(1-phenyl-1*H*-benzo[d]imidazole) (SBFBI) and 2,2'-(spiro[benzo[de]anthracene-7,9'-fluorene]-2',3-diylbis(4,1-phenylene))bis(1-phenyl-1*H*-benzo[d]imidazole) (SAFBI), integrating spirobenzofluorene and benzoimidazole

* Corresponding authors.

E-mail addresses: geziyi@nimte.ac.cn (Z. Ge), ouyangxh@nimte.ac.cn (X. Ouyang), wangsd@suda.edu.cn (S. Wang).

moieties. It is particularly intriguing to compare the electroluminescent properties of SBFBI and SAFBI, both have the same molecular constructing units. We only changed the constitution of spirobenzofluorene core between two benzimidazole units, the emission was found to be changed from sky-blue to deep-blue. Our results provide a way to design and synthesize deep-blue materials based on spirofluorene derivatives. The thermal properties and energy levels were fully investigated. The OLEDs based on SAFBI as the emitting layer achieved a current efficiency of 1.96 cd A⁻¹ and a deep-blue CIE(x,y) of (0.15, 0.10), which was the first time to obtain a deep-blue emitter with spirobenzofluorene derivative in a non-doped system to our knowledge.

2. Experimental

2.1. Materials and measurements

Manipulations involving air-sensitive reagents were performed under an inert atmosphere of dry nitrogen. Commercially available reagents were used without further purification unless otherwise stated. Naphthalene-1,8-diamine, phenylboronic acid, 2-bromo-9H-fluorene-9-one, 9H-fluorene-9-one, naphthalene-1-ylboronic acid, 1-bromo-2-iodobenzene, 2-(4-bromophenyl)-1-phenyl-1H-benzodimidazole were purchased from TCI co. and used as received. 1,8-diiodonaphthalene [15], 1-iodo-8-phenylnaphthalene [16], 3-bromospiro[benzo[de]-anthracene-7,9'-fluorene] [17], 1-(2-bromophenyl)naphthalene, spiro[fluorene-7,9'-benzofluorene], 5-bromospiro[benzo[c]fluorene-7,9'-fluorene] [8], and 1-phenyl-2-(4-(4,4,5,5-tetramethyl-1,3,2-dioxaborolan-2-yl)phenyl)-1H-benzodimidazole [18] were synthesized according to the methods of the reported literature. Melting points were obtained with Shanghai YiCe WRX-4 melting-point apparatus. Fourier transform-infrared (FTIR) spectra were performed using Thermo Nicolet 6700 spectrophotometer. Nuclear magnetic resonance (NMR) spectra were measured on a Bruker DRX-400 spectrometer with chemical shifts reported as ppm (in CDCl₃ or Acetone-d₆, TMS as internal standard). High-resolution mass spectra were obtained from Bruker Esquire LC/Ion Trap Mass Spectrometer and JEOL/HX-110. Elemental analyses were performed with a Perkin-Elmer 2400 II elemental analyzer. UV-vis absorption spectra (UV) were recorded on a Perkin-Elmer Lambda 950 spectrophotometer. Fluorescence (PL) measurements were carried out with a FLS920 spectrophotometer in a solution of 10⁻⁶ mol/L and solid state, respectively. Differential scanning calorimetry (DSC) curves were obtained with Mettler Toledo DSC822 instrument at 20 °C min⁻¹ under nitrogen flushing. Thermogravimetric analyses (TGA) were carried out using a Perkin-Elmer Pyris thermogravimeter under a dry nitrogen gas flow at a heating rate of 10 °C min⁻¹. The electrochemical properties of derivatives was studied through cyclic voltammetry (CV) on a CHI 660D analyzer with a three electrode configuration with a Pt disk as the working electrode of 0.01 cm², a Pt wire as the counter electrode, and an Ag/AgCl as the reference electrode, and in a dichloromethane solution containing 0.1 M of tetrabutylammonium hexafluorophosphate as supporting electrolyte.

2.2. Preparation of 5,9-dibromospiro[benzo[c]fluorene-7,9'-fluorene] (5,9-dBr-SBFF)

5-Bromospiro[benzo[c]fluorene-7,9'-fluorene] (4.01 g, 9.0 mmol) was dissolved in trichloromethane (50 mL) in a two-necked flask; bromine (2.16 g, 13.5 mmol) was then added slowly in a dropwise fashion over a period of 20 min. The mixture was stirred at room temperature, then the reaction mixture was extracted with dichloromethane and water. After the organic layer was evaporated with a rotary evaporator, the resulting powdery

product was purified by column chromatography to give a yellow solid. Yield, 93%. ¹H NMR (400 MHz, Acetone-d₆) δ 9.01 (d, 1H, J = 8.32 Hz), 8.59 (d, 1H, J = 8.32 Hz), 8.35 (d, 1H, J = 8.32 Hz), 8.08 (d, 2H, J = 7.39 Hz), 7.91 (t, 1H, J = 7.39 Hz), 7.81 (t, 1H, J = 7.86 Hz), 7.72 (d, 1H, J = 8.32 Hz), 7.49 (t, 2H, J = 7.39 Hz), 7.20 (t, 2H, J = 7.86 Hz), 7.10 (s, 1H), 6.91 (s, 1H), 6.78 (d, 2H, J = 7.39 Hz).

2.3. Preparation of 2',3-dibromospiro[benzo[de]anthracene-7,9'-fluorene] (2',3-dBr-SBAF)

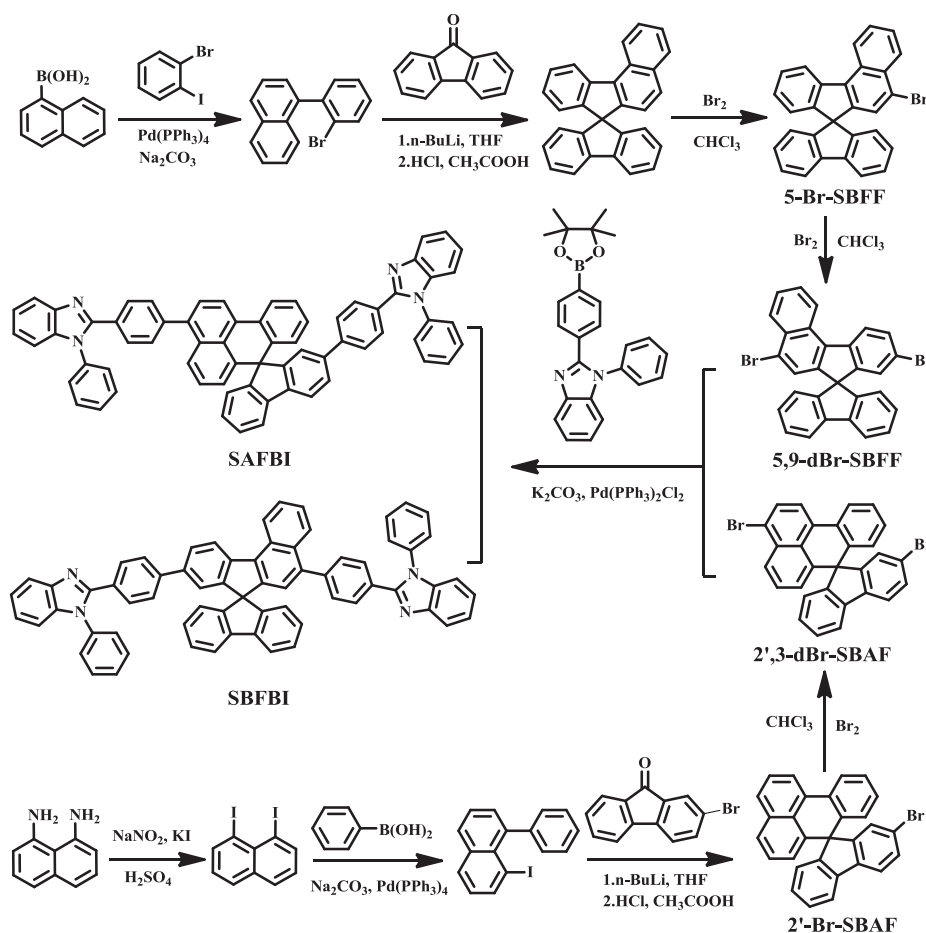
Using a similar approach for 5,9-dBr-SBFF, yellow powder was finally obtained. Yield, 98%. Mp 231 °C. FTIR (KBr, cm⁻¹) 3053, 3023, 739, 765 (aromatic C-H), 1587, 1489, 1463, 1440 (aromatic C=C), 753 (aromatic C-Br). ¹H NMR (400 MHz, CDCl₃) δ 8.19 (d, 1H, J = 7.86 Hz), 8.16–8.10 (m, 2H), 7.95 (d, 1H, J = 8.06 Hz), 7.81 (d, 1H, J = 7.67 Hz), 7.70 (d, 1H, J = 8.06 Hz), 7.49 (dd, 1H, J₁ = 8.15 Hz, J₂ = 1.75 Hz), 7.38 (td, 1H, J₁ = 7.57 Hz, J₂ = 0.78 Hz), 7.35–7.30 (m, 2H), 7.17 (td, 1H, J₁ = 7.57 Hz, J₂ = 0.97 Hz), 7.05–7.01 (m, 2H), 6.94 (d, 1H, J = 7.67 Hz), 6.68 (d, 1H, J = 7.28 Hz), 6.51 (dd, 1H, J₁ = 8.01 Hz, J₂ = 0.58 Hz). HRMS (m/z): calcd for (M⁺+H) C₂₉H₁₇Br₂ (524.9598), found 524.9582.

2.4. Synthesis of 2,2'-(spiro[benzo[c]fluorene-7,9'-fluorene]-5,9-diylbis(4,1-phenylene))bis(1-phenyl-1H-benzodimidazole) (SBFBI)

1-phenyl-2-(4-(4,4,5,5-tetramethyl-1,3,2-dioxaborolan-2-yl)phenyl)-1H-benzodimidazole (1.75 g, 4.4 mmol), 5,9-dBr-SBFF (1.0 g, 2.0 mmol), bis(triphenyl phosphine)palladium(II)chloride (0.20 g, 0.28 mmol) and toluene (100 mL) were stirred in a three-necked flask for 30 min. To the above solution was added potassium carbonate (2 M, 20 mL) and anhydrous ethanol (30 mL). The resulting solution was refluxed 2 days at 105 °C. The reaction mixture was extracted with dichloromethane and water. After the organic layer was evaporated with a rotary evaporator, the resulting powdery product was purified by column chromatography to give a white solid. Yield, 45%. Mp 385 °C. FTIR (KBr, cm⁻¹) 3064, 3053, 3038, 818, 756, 742 (aromatic C-H), 1597, 1499, 1450, 1406 (aromatic C=C), 1476 (C=N), 1260 (C-N). ¹H NMR (400 MHz, CDCl₃) δ 8.95 (d, 1H, J = 8.51 Hz), 8.53 (d, 1H, J = 8.19 Hz), 8.00–7.94 (m, 3H), 7.89 (d, 2H, J = 7.53 Hz), 7.79–7.73 (m, 2H), 7.66–7.23 (m, 27H), 7.13 (td, 2H, J₁ = 7.61 Hz, J₂ = 0.74 Hz), 7.00 (d, 1H, J = 1.64 Hz), 6.79 (d, 2H, J = 7.53 Hz), 6.75 (s, 1H). ¹³C NMR (100 MHz, CDCl₃): δ 151.4, 151.3, 151.2, 150.7, 147.7, 147.3, 142.4, 142.3, 142.3, 142.2, 142.1, 140.0, 138.6, 136.9, 136.7, 136.4, 136.3, 135.9, 132.0, 130.3, 130.2, 130.1, 129.9, 129.8, 129.2, 129.1, 128.0, 127.4, 127.4, 127.3, 127.1, 127.0, 126.9, 125.9, 124.2, 124.1, 124.0, 123.9, 123.8, 123.7, 123.4, 122.8, 122.3, 120.2, 119.3, 119.2, 110.7. ESI-MS (m/z): 904.5 (M⁺+H). HRMS (m/z): calcd for (M⁺+H) C₆₇H₄₃N₄ (903.3409), found 903.3417. Anal. Calcd for C₆₇H₄₂N₄: C, 89.11; H, 4.69; N, 6.20; Found: C, 89.03; H, 4.63; N, 6.21.

2.5. Synthesis of 2,2'-(spiro[benzo[de]anthracene-7,9'-fluorene]-2',3-diylbis(4,1-phenylene))bis(1-phenyl-1H-benzodimidazole) (SAFBI)

The synthesis of SAFBI is similar to that of SBFBI by a Suzuki coupling reaction, white powder was finally obtained. Yield, 87%. Mp > 300 °C. FTIR (KBr, cm⁻¹) 3060, 3034, 831, 762, 748 (aromatic C-H), 1598, 1499, 1449, 1402 (aromatic C=C), 1478 (C=N), 1262 (C-N). ¹H NMR (400 MHz, CDCl₃) δ 8.33 (d, 1H, J = 7.85 Hz), 8.26 (d, 1H, J = 7.91 Hz), 8.02 (d, 1H, J = 8.01 Hz), 7.97 (d, 1H, J = 7.91 Hz), 7.92 (d, 1H, J = 8.01 Hz), 7.86 (d, 1H, J = 7.56 Hz), 7.77 (d, 2H, J = 8.11 Hz), 7.74 (dd, 1H, J₁ = 8.42 Hz, J₂ = 0.82 Hz), 7.65 (dd, 1H, J₁ = 7.91 Hz, J₂ = 1.54 Hz), 7.62–7.54 (m, 8H), 7.52–7.39 (m, 9H),



Scheme 1. The synthetic routes to SBFBI and SAFBI.

7.37–7.29 (m, 7H), 7.23 (d, 2H, $J = 8.21$ Hz), 7.18–7.11 (m, 2H), 7.01 (t, 1H, $J = 7.70$ Hz), 6.96 (d, 1H, $J = 7.49$ Hz), 6.68 (dd, 1H, $J_1 = 7.29$ Hz, $J_2 = 0.82$ Hz), 6.57 (dd, 1H, $J_1 = 8.00$ Hz, $J_2 = 1.03$ Hz). ^{13}C NMR (100 MHz, CDCl_3): δ 157.6, 157.5, 151.7, 151.4, 142.5, 142.2, 140.2, 140.1, 139.3, 138.7, 138.5, 137.3, 137.0, 136.8, 136.7, 136.5, 131.8, 131.6, 130.2, 130.1, 130.0, 129.8, 129.6, 129.5, 129.0, 128.9, 128.6, 128.6, 128.3, 127.8, 127.6, 127.5, 127.4, 127.4, 126.9, 126.8, 126.6, 125.5, 125.3, 124.6, 124.1, 123.8, 123.6, 123.5, 123.3, 120.5, 120.3, 119.5, 119.3, 119.1, 110.6, 110.6. HRMS (m/z): calcd for ($\text{M}^+ + \text{H}$) $\text{C}_{67}\text{H}_{43}\text{N}_4$ (903.3409), found 903.3349. Anal. Calcd for $\text{C}_{67}\text{H}_{42}\text{N}_4$: C, 89.11; H, 4.69; N, 6.20; Found: C, 89.04; H, 4.65; N, 6.21.

2.6. Device fabrication and testing

SBAFI and SBFBI were purified by vacuum sublimed and the purity of the materials is above 99% before the OLEDs fabrication. The ITO-coated glass substrates were routinely cleaned and subsequently treated with UV-ozone. The EL devices were fabricated

by vacuum deposition of the materials at 10^{-6} Torr onto ITO glass with a sheet resistance of $6 \Omega \text{ cm}^{-2}$. All of the organic layers and inorganic layers were prepared in sequence by vacuum deposition. The electroluminescence spectra and Commission Internationale De L'Eclairage (CIE) coordination of these devices were measured by a PR655 spectra scan spectrometer. The luminance-current and density-voltage characteristics were recorded simultaneously with the measurement of the EL spectra by combining the spectrometer with a programmable voltage–current source. All measurements were carried out at room temperature under ambient conditions.

3. Results and discussion

3.1. Synthesis and characterization

The synthetic routes and molecular structures of SAFBI and SBFBI are illustrated in Scheme 1. Some starting materials were synthesized according to the reported methods of literature [8,15–

Table 1
Thermal properties, optical properties and energy levels of SBFBI and SAFBI.

Compounds	T_m/T_d [$^{\circ}\text{C}$]	λ_{max} Abs ^a [nm]	λ_{max} PL ^{a,b} [nm]	HOMO/LUMO ^{exp} ($E_{\text{g}}^{\text{opt}}$) ^c [eV]	HOMO/LUMO ^{cal} ($E_{\text{g}}^{\text{cal}}$) ^d [eV]
SBFBI	385/524	359	440/461	–5.62/–2.62 (3.00)	–5.22/–1.68 (3.54)
SAFBI	–/426	325	440/456	–5.62/–2.51 (3.11)	–5.28/–1.55 (3.73)

^a Measured in CHCl_3 .

^b Measured in solid film on quartz plates.

^c Estimated based on absorption onset and cyclic-voltammetry. $E_{\text{HOMO}} = -(qE_{\text{ox}} + 4.4)$ eV, $E_{\text{LUMO}} = E_{\text{g}}^{\text{opt}} + E_{\text{HOMO}}$.

^d DFT calculation with B3LYP/6-31G.

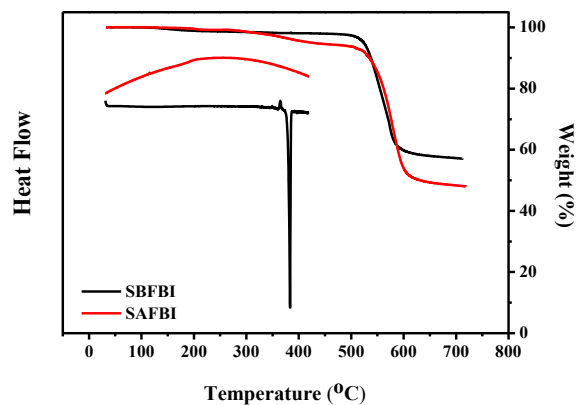


Fig. 1. TGA thermograms of SBFBI and SAFBI recorded at a heating rate of $10\text{ }^{\circ}\text{C min}^{-1}$ and DSC traces of SBFBI and SAFBI recorded at a heating rate of $20\text{ }^{\circ}\text{C min}^{-1}$.

18]. The 2',3-dBr-SBAF or 5,9-dBr-SBFF were obtained by reaction with bromine and 2',3-dBr-SBAF or 5,9-dBr-SBFF were obtained in good yield. Bromination reactions were employed in the synthesis of the intermediates with a yield of over 90%. The target compounds were obtained by the bromides reacting with boronate compounds through Suzuki coupling reaction in aqueous potassium carbonate solution. The compounds were purified by column chromatography using common solvent systems. The chemical structures of SAFBI and SBFBI were confirmed by ^1H NMR and ^{13}C NMR. The results of mass spectrometry also supported the formation of the two target materials and matched well with the calculated data. Compounds SAFBI and SBFBI had good solubility in common organic solvents so that they could be easily purified by column chromatography to high purity for spectroscopic characterization and OLEDs application.

3.2. Thermal properties

The thermal properties of SBFBI and SAFBI were measured by differential scanning calorimetry (DSC) and thermogravimetric

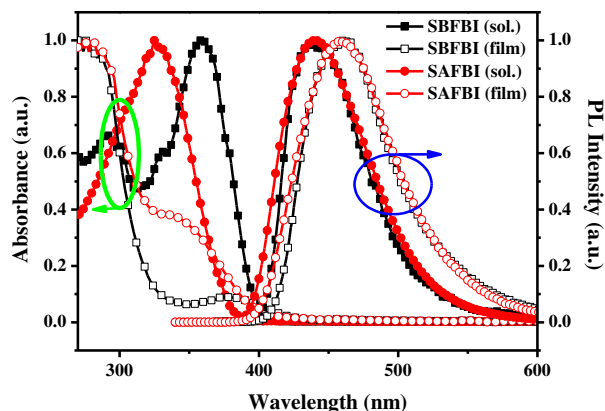


Fig. 3. UV absorption and PL spectra of SBFBI and SAFBI.

analysis (TGA) under a nitrogen atmosphere, and their thermal data are shown in Table 1 and Fig. 1. In the DSC, no obvious glass transition temperatures (T_g) were observed for them and they did not show any melting transition even when SAFBI was heated up to $420\text{ }^{\circ}\text{C}$, while endothermic melting transition temperature (T_m) appeared obviously at $385\text{ }^{\circ}\text{C}$ for SBFBI. These results indicate that highly twisted structures, due to the different constitution of SAFBI compared to SBFBI, might mitigate the intermolecular interactions of SAFBI in the solid state [19]. From the TGA results, SBFBI and SAFBI exhibited decomposition (T_d , corresponding to 5% weight loss) as high as $524\text{ }^{\circ}\text{C}$ and $426\text{ }^{\circ}\text{C}$, respectively. Such high T_d values indicate that these molecules are stable and have the potential to be fabricated into devices by vacuum thermal evaporation technology [20–22].

3.3. Theoretical calculations

To understand the electronic structures of these compounds, the molecular geometry and frontier molecular orbitals were calculated at B3LYP/6-31G (d,p) level by using DFT in Gaussian 03

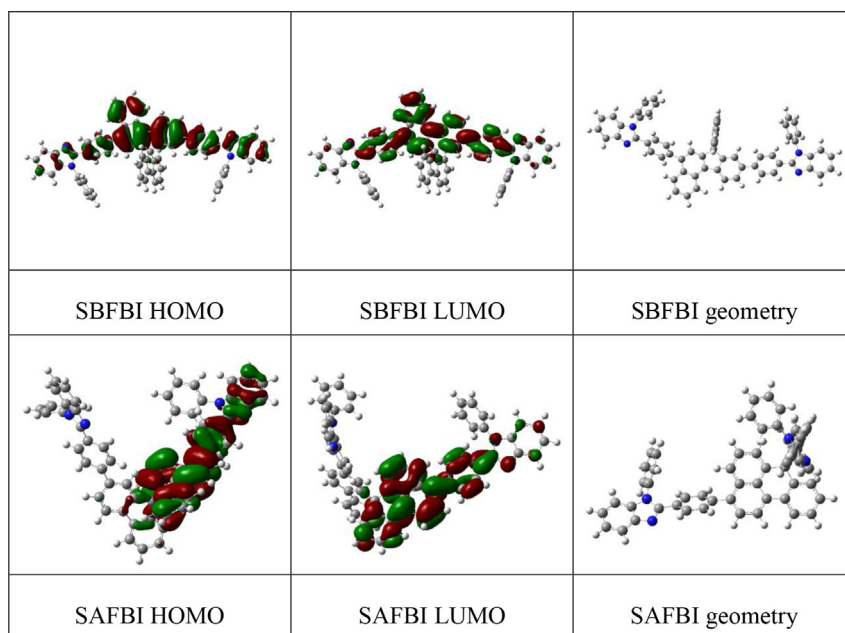


Fig. 2. Molecular orbital distribution and optimized geometries of SBFBI and SAFBI.

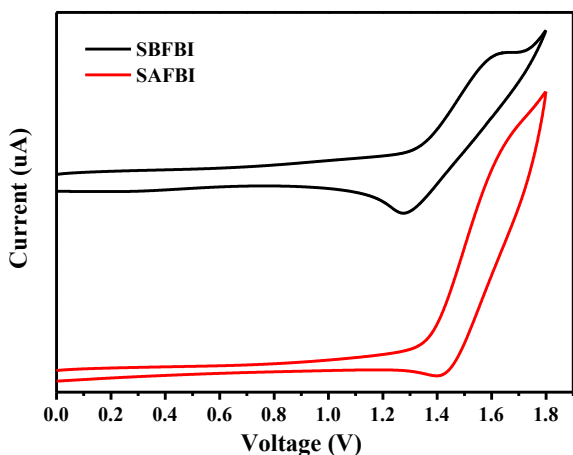


Fig. 4. Cyclic voltammograms of compounds SBFBI and SAFBI in CH_2Cl_2 .

program. As shown in Fig. 2, the HOMO and LUMO of SBFBI were delocalized in the SBFF and two benzimidazole units, while the HOMO and LUMO were delocalized in the SBAF and one benzimidazole moiety. Compared with SBFBI, the tilted angle of the two benzimidazoles for SAFBI is almost 90° because of the steric hindrance. Consequently, the non-planar geometry of SAFBI efficiently prevents the recrystallization due to the large torsional stresses, which can induce the formation of either an exciplex or excimer [23].

3.4. Photophysical and electrochemical properties

The UV-vis absorption and PL spectra of SBFBI and SAFBI in diluted CHCl_3 solutions and in the solid film spin-coated on quartz plates were explored as shown in Fig. 3. The photophysical data of the compounds are summarized in Table 1. SBFBI showed a UV-vis absorption maximum at 359 nm, whereas SAFBI showed a UV absorption maximum at 325 nm originated from the $\pi-\pi^*$ transition of the spiro[benzoanthracene-fluorene] core in CHCl_3 solution [17]. For the fluorescence spectra of SBFBI and SAFBI, they both emit blue fluorescence peaking at 440 nm in dilute CHCl_3 solution. In the film state, the emissions from these two molecules show a red shift but still localized in the blue spectral region 461 nm for SBFBI, and 456 nm for SAFBI, respectively. Additionally, it is worth noting that the PL spectrum of SBFBI is more red-shifted compared with SAFBI. It can be attributed to the constitution of SAFBI with a large steric hindrance, which prevents close molecular packing in the solid film [19].

Cyclic voltammetry analysis were carried out to measure the HOMO values of the synthesized compounds, and the results are

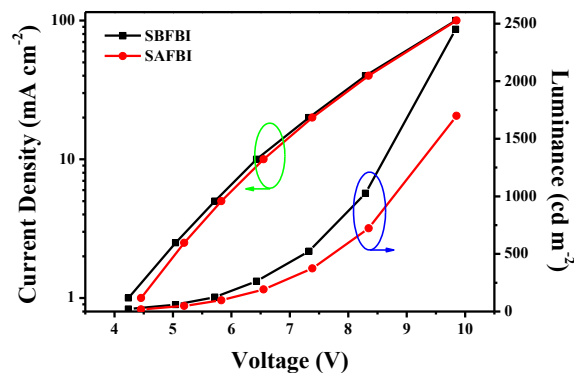


Fig. 6. Current density-voltage-luminance characteristics of SBFBI and SAFBI devices.

shown in Table 1 and Fig. 4. HOMO values are calculated from as $\text{HOMO} = -([E_{\text{onset}}]_{\text{ox}} + 4.4)$ [24]. Both HOMO values of SBFBI and SAFBI are -5.62 eV. Such a low HOMO energy level greatly reduced the energy barrier for hole injection from indium tin oxide (ITO) to the emissive derivatives. The energy band gaps of the compounds are estimated by analyzing absorption edge with a plot of UV-vis curve. The energy band gaps of SAFBI and SBFBI are found to be 3.11 eV and 3.00 eV, respectively. The LUMO levels of SAFBI and SBFBI calculated by $\text{HOMO} + E_{\text{g}}^{\text{opt}}$ are -2.51 eV and -2.62 eV. It was found that SAFBI showed a relatively higher LUMO energy with a larger band gap due to the distorted π -conjugation of SAFBI [25].

3.5. Electroluminescent properties

Nondoped OLED devices were fabricated to investigate the EL performances of SBFBI and SAFBI, the structure of devices is ITO/MoO₃ (10 nm)/NPB (80 nm)/TCTA (5 nm)/SBFBI or SAFBI (20 nm)/TPBi (40 nm)/LiF (1 nm)/Al (100 nm). Indium tin oxide (ITO) and Al were utilized as anode and cathode, MoO₃ was as a hole injecting layer, *N,N'*-bis(naphthalene-1-yl)-*N,N'*-bis(phenyl)-benzidine (NPB) was as a hole transporting layer, 4,4',4''-tri(*N*-carbazolyl)benzene (TCTA) was as an electron blocking layer, 1,3,5-tri(phenyl-2-benzimidazolyl)benzene (TPBi) was as an electron transporting and hole blocking layer, and LiF was used as an electron injecting layer. The EL spectra of SBFBI or SAFBI devices at different current density are shown in Fig. 5. The maximum emission λ_{max} of both SBFBI and SAFBI are located at 436 nm, and the FWHM values are 85 nm and 54 nm. There is a 25 nm blue-shift for SBFBI and a 20 nm blue-shift for SAFBI. It is common that the ~ 20 nm shift is observed in OLEDs [26,27]. For the EL spectra of SBFBI device at different current density, there is a slight difference in the intensity of the shoulder at ~ 500 nm. This phenomenon should be ascribed to the

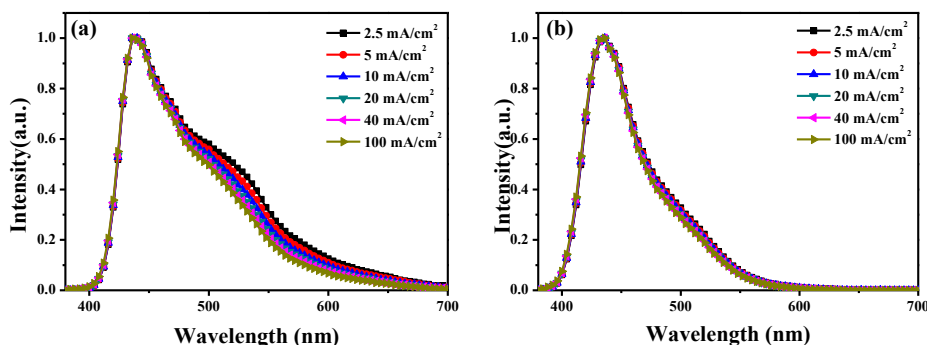


Fig. 5. Normalized EL spectra for the blue FLOLEDs with SBFBI (a) and SAFBI (b).

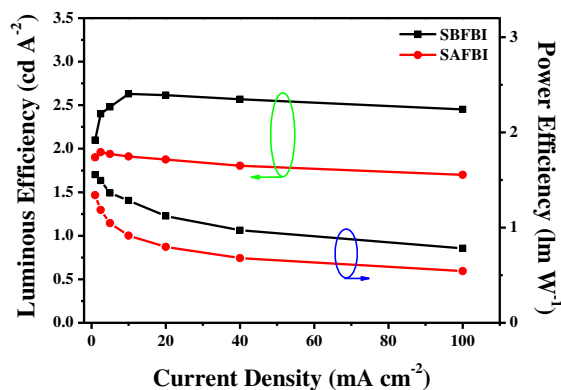


Fig. 7. Luminous efficiency curves and power efficiency curves versus current density for SBFBI and SAFBI devices.

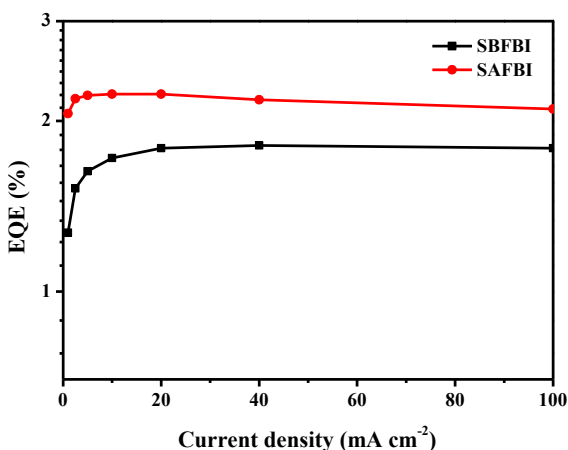


Fig. 8. The external quantum efficiency of SBFBI and SAFBI based FLOLEDs.

electromer formation of SBFBI, since there is no evidence of excimer formation from the film and solution PL spectra [21]. Fig. 6 shows the current density-voltage-luminance characteristics of the devices.

As shown in Fig. 7, the maximum luminance efficiencies for SBFBI and SAFBI are 2.63 cd A⁻¹ and 1.96 cd A⁻¹, and the maximum power efficiencies are 1.56 lm W⁻¹ and 1.34 lm W⁻¹, respectively. The external quantum efficiencies (EQE) maximum of these non-doped FLOLEDs are 1.81% for SBFBI and 2.23% for SAFBI (see Fig. 8.). When the current density is at 20 mA cm⁻², the CIE coordinates (x, y) of SBFBI- and SAFBI-based on devices are found to be (0.18, 0.20) and (0.15, 0.10), which is close to the blue standards (0.14, 0.08) of NTSC. As expected, SAFBI showed deep-blue emission, while SBFBI showed sky-blue emission. The effect on the change in CIE coordinates of SBFBI device from the shoulder at ~500 nm can be neglected because the intensity of the shoulder at ~500 nm only changes a little as increasing the current density. Especially, the

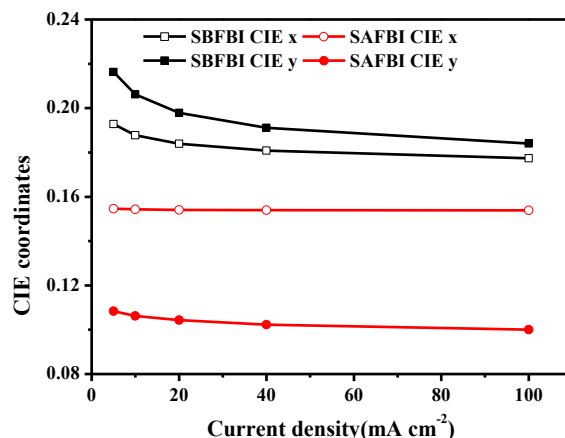


Fig. 9. CIE coordinates deviation of EL spectra in response to the current change of SBFBI and SAFBI EL devices.

shoulder at ~500 nm in the EL spectra of SBFBI device is almost disappeared at high current density. However, the CIE coordinates (x, y) of SBFBI- and SAFBI-based on devices are found to be (0.18, 0.18) and (0.15, 0.10) when the current density is at 100 mA cm⁻². We can confirm the CIE coordinates difference between these two devices results from different FWHM of two EL spectra, which contributes to the much more twisted molecular structure of the SAFBI [23]. The EL properties of the devices for SBFBI and SAFBI are summarized in Table 2.

Notably, the CIE values deviation of SAFBI device is negligible (x = 0.001, y = 0.008) with the current density increasing from 5 mA cm⁻² to 100 mA cm⁻² (see Fig. 9). According to the color stability of SAFBI-based device, we can confirm that the energy levels of SAFBI match well with neighboring layers, and the charge carrier recombination at the emitting layer is efficient at all current density [23].

4. Conclusion

Two benzimidazole-attached spiro[benzofluorene] derivatives (SBFBI and SAFBI) were successfully designed and synthesized for blue emitters in nondoped OLEDs. The nondoped, blue fluorescent organic light-emitting diodes were fabricated with the structure of ITO/MoO₃ (10 nm)/NPB (80 nm)/TCTA (5 nm)/SBFBI or SAFBI (20 nm)/TPBi (40 nm)/LiF (1 nm)/Al (100 nm). The devices fabricated with SAFBI exhibited efficiencies of 1.96 Cd/A, 1.34 lm/W as well as a deep-blue emission with CIE coordinates of (0.15, 0.10) and little efficiency roll-off and color change at high brightness. It is particularly intriguing to compare the electroluminescent properties of SBFBI and SAFBI, both have the same molecular constructing units. We only changed the constitution of spirobenzofluorene core between two benzoimidazole units, the emission was found to be changed from sky-blue to deep-blue. Our results provide a way to design and synthesize deep-blue materials based on spirofluorene derivatives.

Table 2
Electroluminescent characteristics of SBFBI and SAFBI.

Devices	CIE ^a [x, y]	λ_{\max} EL [nm]	LE _{max} [cd A ⁻¹]	PE _{max} [lm W ⁻¹]	EQE _{max} [%]	Devices performance at 20 mA cm ⁻²		
						LE [cd A ⁻¹]	PE [lm W ⁻¹]	EQE [%]
SBFBI	0.18, 0.20	436	2.63	1.56	1.81	2.62	1.12	1.79
SAFBI	0.15, 0.10	436	1.96	1.34	2.23	1.88	0.80	2.23

^a Values collected at 20 mA cm⁻².

Acknowledgments

This work was financial supported from National Natural Science Foundation of China (21102156, 51273209), Ningbo International Cooperation Foundation (2012D10009, 2013D10013), the Open Fund of the State Key Laboratory of Luminescent Materials and Devices (South China University of Technology) (2013-SKLLMD-02) and the External Cooperation Program of the Chinese Academy of Sciences (No. GJHZ1219).

References

- [1] Li WJ, Liu DD, Shen FZ, Ma DG, Wang ZM, Feng T, et al. A twisting donor-acceptor molecule with an intercrossed excited state for highly efficient, deep-blue electroluminescence. *Adv Funct Mater* 2012;22:2797–803.
- [2] Shin MG, Kim SO, Park HT, Park SJ, Yu HS, Kim YH, et al. Synthesis and characterization of ortho-twisted asymmetric anthracene derivatives for blue organic light emitting diodes (OLEDs). *Dyes Pigments* 2012;92:1075–82.
- [3] Zhang P, Dou W, Ju ZH, Yang LZ, Tang XL, Liu WS, et al. A 9,9'-bianthracene-cored molecule enjoying twisted intramolecular charge transfer to enhance radiative-excitons generation for highly efficient deep-blue OLEDs. *Org Electron* 2013;14:915–25.
- [4] Hu JY, Pu YJ, Yamashita Y, Satoh F, Kawata S, Katagiri H, et al. Excimer-emitting single molecules with stacked π -conjugated groups covalently linked at the 1,8-positions of naphthalene for highly efficient blue and green OLEDs. *J Mater Chem C* 2013;1:3871–8.
- [5] Kamino BA, Chang YL, Lu ZH, Bender TP. Phthalonitrile based fluorophores as fluorescent dopant emitters in deep-blue OLEDs: approaching the NTSC standard for blue. *Org Electron* 2012;13:1479–85.
- [6] Xing X, Xiao LX, Zheng LL, Hu SY, Chen ZJ, Qu B, et al. Spirobifluorene derivative: a pure blue emitter ($CIE_y \approx 0.08$) with high efficiency and thermal stability. *J Mater Chem* 2012;22:15136–40.
- [7] Chang YC, Yeh SC, Chen YH, Chen CT, Lee RH, Jeng RJ. New carbazole-substituted anthracene derivatives based non-doped blue light-emitting devices with high brightness and efficiency. *Dyes Pigments* 2013;99:577–87.
- [8] Jeon SO, Jeon YM, Kim JW, Lee CW, Gong MS. Blue organic light-emitting diode with improved color purity using 5-naphthyl-spiro[fluorene-7,9'-benzofluorene]. *Org Electron* 2008;9:522–32.
- [9] Liu F, Xie LH, Tang C, Liang J, Chen QQ, Peng B, et al. Facile synthesis of spirocyclic aromatic hydrocarbon derivatives based on o-halobiaryl route and domino reaction for deep-blue organic semiconductors. *Org Lett* 2009;11:3850–3.
- [10] Lee CW, Jang JG, Gong MS. Deep blue fluorescent host materials based on spirobenzofluorene-fluorene dimers and their properties. *Dyes Pigments* 2013;98:471–8.
- [11] Jeong SJ, Kim MK, Kim SH, Hong JI. Efficient deep-blue emitters based on triphenylamine-linked benzimidazole derivatives for nondoped fluorescent organic light-emitting diodes. *Org Electron* 2013;14:2497–504.
- [12] Linton KE, Fisher AL, Pearson C, Fox MA, Pålsson LO, Bryce MR, et al. Colour tuning of blue electroluminescence using bipolar carbazole-oxadiazole molecules in single-active-layer organic light emitting devices (OLEDs). *J Mater Chem* 2012;22:11816–25.
- [13] Lee YH, Wu TC, Liaw CW, Wen TC, Feng SW, Lee JJ, et al. Nondoped active layer, benzo[k]fluoranthene-based linear acenes, for deep blue- to green-emissive organic light-emitting diodes. *Org Electron* 2013;14:1064–72.
- [14] Zhang Y, Lai SL, Tong QX, Lo MF, Ng TW, Chan MY, et al. High efficiency nondoped deep-blue organic light emitting devices based on imidazole- π -triphenylamine derivatives. *Chem Mater* 2012;24:61–70.
- [15] Weimar M, Dürner G, Bats JW, Göbel MW. Enantioselective synthesis of (+)-estrone exploiting a hydrogen bond-promoted Diels-Alder reaction. *J Org Chem* 2010;75:2718–21.
- [16] Lejeune M, Grosshans P, Berclaz T, Sidorenkova H, Besnard C, Pattisoncd P, et al. Role of the aromatic bridge on radical ions formation during reduction of diphosphaalkenes. *New J Chem* 2011;35:2510–20.
- [17] Kim JY, Lee CW, Jang JG, Gong MS. Orange phosphorescent organic light-emitting diodes using new spiro[benzanthracene-fluorene]-type host materials. *Dyes Pigments* 2012;94:304–13.
- [18] Yang XH, Zheng SJ, Bottger R, Chae HS, Tanaka T, Li S, et al. Efficient fluorescent deep-blue and hybrid white emitting devices based on carbazole/benzimidazole compound. *J Phys Chem C* 2011;115:14347–52.
- [19] Park H, Lee J, Kang I, Chu HY, Lee JI, Kwon SK, et al. Highly rigid and twisted anthracene derivatives: a strategy for deep blue OLED materials with theoretical limit efficiency. *J Mater Chem* 2012;22:2695–700.
- [20] Zhang XQ, Chi ZG, Xu BJ, Li HY, Yang ZY, Li XF, et al. Synthesis of blue light emitting bis(triphenylethylene) derivatives: a case of aggregation-induced emission enhancement. *Dyes Pigments* 2011;89:56–62.
- [21] Huang JH, Su JH, Li X, Lam MK, Fung KM, Fan HH, et al. Bipolar anthracene derivatives containing hole- and electron-transporting moieties for highly efficient blue electroluminescence devices. *J Mater Chem* 2011;21:2957–64.
- [22] Tang S, Li WJ, Shen FZ, Liu DD, Yang B, Ma YG. Highly efficient deep-blue electroluminescence based on the triphenylamine-cored and peripheral blue emitters with segregative HOMO-LUMO characteristics. *J Mater Chem* 2012;22:4401–8.
- [23] Cho I, Kim SH, Kim JH, Park S, Park SY. Highly efficient and stable deep-blue emitting anthracene-derived molecular glass for versatile types of non-doped OLED applications. *J Mater Chem* 2012;22:123–9.
- [24] Zhang H, Wan X, Xue X, Li Y, Yu A, Chen Y. Selective tuning of the HOMO-LUMO gap of carbazole-based donor-acceptor-donor compounds toward different emission colors. *Eur J Org Chem* 2010;9:1681–7.
- [25] Wan W, Du HL, Wang J, Le YP, Jiang HZ, Chen H, et al. Novel blue luminescent materials for organic light-emitting diodes based on C9-fluorenyl anthracenes. *Dyes Pigments* 2013;96:642–52.
- [26] Liang ZQ, Zeng ZC, Zou DC, Wang XM, Tao XT. Novel 4-(2,2-diphenyl-vinyl)-phenyl substituted pyrene derivatives as efficient emitters for organic light-emitting diodes. *Org Electron* 2012;13:2898–904.
- [27] Feng XJ, Chen SF, Yong Ni, Wong MS, Lam MM, Cheah KW, et al. Fluorene derivatives for highly efficient non-doped single-layer blue organic light-emitting diodes. *Org Electron* 2014;15:57–64.